Srivastava, S. P., Arthur, M., Clement, B., et al., 1989
Proceedings of the Ocean Drilling Program, Scientific Results, Vol. 105

8. ANALYSIS OF SEDIMENTARY FACIES, CLAY MINERALOGY, AND GEOCHEMISTRY OF THE PALEOGENE SEDIMENTS OF SITE 647, LABRADOR SEA[1]

O. B. Nielsen,[2] M. Cremer,[3] R. Stein,[4] F. Thiébault,[5] and H. Zimmerman[6]

ABSTRACT

Claystones immediately overlying the early Eocene age ocean-floor basalt, cored at Ocean Drilling Program (ODP) Site 647, underwent hydrothermal and thermal alterations originating from the basalt, which resulted in changes in both the mineralogical and chemical composition of the sediments. Chlorites and higher magnesium and iron concentrations were found in the lowermost sediment sequence. Upcore, changes in the bulk chemical composition of the sediments become smaller, when compensated for variations in the carbonate content originating from biogenic and authigenic components. Chlorite disappears upcore, but still only part of the swelling clay minerals have survived the thermal influence. Thirty meters above the basalt, the clay mineralogy and chemical composition become uniform throughout the Paleogene section. Iron-rich smectites (i.e., nontronitic types), totally dominate the clay mineral assemblage. Biogenic components, responsible for the dominant part of the calcite and cristobalite contents, vary in amount in the upper part, and so do the authigenic carbonate and sulfide contents. Detrital components, such as kaolinite, illite, quartz, and feldspars, make up a very small proportion of the sediment record. The nontronitic smectites are believed to be authigenic, formed by a supply of iron from the continuous formation of ocean-floor basalt in the ridge area that reacted with the detrital and biogenic silicates and alumina silicates.

INTRODUCTION

Sediments from the Paleogene section (135.4–699 mbsf) of Site 647 in the Labrador Sea (Fig. 1) were analyzed for texture, bulk sediment mineralogy, mineralogy of the clay fraction, and whole-rock geochemistry to determine the depositional and diagenetic history of these sediments.

Specifically, the objectives of this study are (1) to evaluate the abundance of detrital and authigenic constituents; (2) to determine the provenance of the nonbiogenic detrital fraction; and (3) to study the hydrothermal/thermal effect of the underlying basalt (at 699 mbsf) on these sediments.

The Paleogene section cored at Site 647 consists of mostly hemipelagic sediments of Eocene and early Oligocene age. These sediments are divided into two lithologic units: lithologic Units III and IV (Srivastava, Arthur, et al., 1987). Lithologic Unit III was further subdivided into three subunits, Subunits IIIA, IIIB, and IIIC. The criteria for these subdivisions are differences in amount and composition of the biogenic components, which include both calcareous particles (mainly foraminifers and nannofossils) and siliceous particles (diatoms and sponge spicules). Unit IV consists entirely of claystones.

METHODS

A total of 42 samples was analyzed in the following manner:

1. Grain-size distribution. Analyses were performed by combining wet sieving (>63-μm fraction) and settling in Andreassen tubes (<63-μm fraction).
2. Bulk sediment chemistry. The contents of calcium, magnesium, manganese, iron, sodium, and aluminum were obtained by atomic absorption (Perkin Elmer 5000) on extracts produced by total dissolution in HF, and the carbon and organic carbon contents were determined in a LECO induction furnace.
3. Bulk sediment mineralogy. The bulk samples were dried at 105°C, ground in an agate mortar, and mounted with random orientation in an aluminum sample holder. The samples were X-rayed from 2–65° 2θ with a speed of 1.8° 2θ/min using copper-k α radiation on a Philips PW 1710 X-ray diffractometer (XRD) with automatic divergence slit, graphite monochromator, and an automatic sample changer. The minerals of the bulk samples were identified and quantified using the peak heights of selected reflections (Schultz, 1964).
4. Clay mineralogy. The clay fraction (<2-μm fraction) was obtained by repeated decanting from an aqueous suspension, followed by centrifugation. Oriented smear-slide preparations were produced on glass plates (Gibbs, 1971). The samples were X-rayed from 2–65° 2θ with a speed of 1.8° 2θ/min using copper-k α radiation on a Philips PW 1710 XRD with automatic divergence slit, graphite monochromator, and an automatic sample changer. Records were made of air dried, of glycollated (24 hr at 60°C), and of heated (500° and 550°C for 2 hr) preparations, respectively. The clay minerals were determined according to Brindley and Brown (1980) and quantified using peak areas of the basal reflections from the glycollated preparations (see Schultz, 1964; Biscaye, 1965; and Johns et al., 1954). The distinction between kaolinite and chlorite was conducted following the methods described by Schultz (1964). The nonclay minerals of the clay-sized fraction were identified and quantified using the peak heights of selected reflections (Schultz, 1964).

RESULTS

Grain Size

The early Eocene sediments contain approximately equal amounts of silt and clay (Fig. 2, Table 1), while the remaining Eocene deposits are richer in clay. The most fine-grained interval is found in the middle of the late Eocene. During the upper part of the late Eocene and Oligocene, the silt content, and consequently the median grain size, increased and the amount of clay-sized particles decreased. The sand content is very low in all samples, except in the uppermost sample, which is from the late Pliocene section. Detrital grains of quartz and feldspar are frequently present in the late Pliocene, in contrast to the under-

---

[1] Srivastava, S. P., Arthur, M., Clement, B., et al., 1989. *Proc. ODP, Sci. Results*, 105: College Station, TX (Ocean Drilling Program).

[2] Department of Geology, Aarhus University, DK-8000 Aarhus C, Denmark.

[3] Departement de Géologie et Océanographie, Université de Bordeaux 1, Avenue des Facultés, 33405 Talence Cedex, France.

[4] Institut für Geowissenschaften und Lithosphärenforschung, Universität Giessen, Senckenbergstrasse 3, D-6300 Giessen, Federal Republic of Germany.

[5] Sciences de la Terre, Université de Lille 1, 59655 Villeneuve D'Ascq Cedex, France.

[6] Division of Polar Programs, National Science Foundation, Washington, DC 20550.

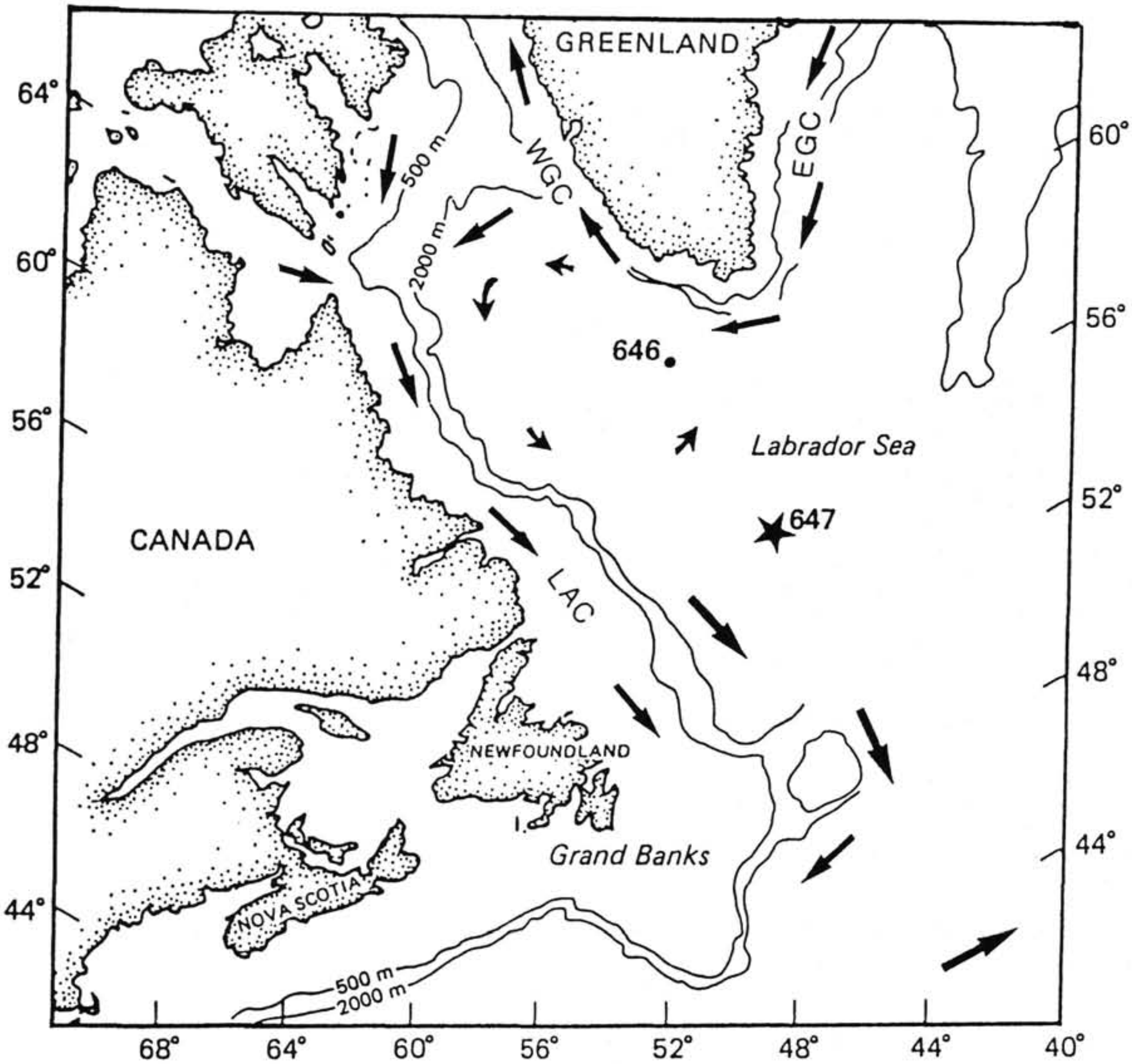

Figure 1. Location map for Site 647. *LAC* = Labrador Current; *EGC* = East Greenland Current; *WGC* = West Greenland Current.

lying sequence, where the few sand grains are predominantly diagenetic or biogenic in origin.

Bulk Mineralogy

Clay minerals and carbonates are the most dominant mineral groups in the entire sequence (Fig. 3, Table 2). Calcite is the most frequent carbonate mineral, but the calcite shows varying degrees of iron, magnesium, and manganese substitution for calcium (see Arthur et al., this volume; Bohrmann and Thiede, this volume). The sample at 650 mbsf represents the most manganese-rich example of these diagenetically altered carbonates found in this study. Zeolites are found only in the Miocene condensed sequence (lithologic Unit II). Cristobalite is found mainly in the interval from 290 to 310 mbsf (see also Bohrmann and Stein, this volume). Pyrite is present sporadically in one-half of the samples, and pyrite concretions are found only from 621 to 630 mbsf. Feldspars and quartz are found in all samples with only few variations throughout the sequence, except in the upper part, where the contents increase parallel to the coarsening trend.

Clay Minerals

Smectite is the most dominant component of the clay minerals in the clay fraction (Fig. 4, Table 3). The (060) reflection on the bulk diffractograms has a position of about 1.5090 Å, which indicates a dioctahedral type of crystal lattice. Illite makes up 10% to 20% of the components, with higher values in the lowermost sample just above the basalt and in the pyritic interval from 621 to 630 mbsf. Kaolinite is present, with contents normally less than 10%, except in the upper part, where the content increases upward from early Oligocene. Chlorite is found only in the lowermost sample, which has a value of 12%, and in the sample at 223 mbsf, with 1%. In the upper part of Site 647, chlorite is present sporadically, but never exceeds 1%. Mixed-layer clay minerals of smectite/illite are present in small and variable amounts throughout the section. The content is relatively high in the early Eocene, relatively small in the middle and late Eocene, and seems to increase upward from early Oligocene.

Geochemistry

Total organic carbon (TOC) is between 0.2% and 0.6% (Fig. 5, Table 4), with a tendency to increase slightly upward. The carbonate contents, calculated from the LECO analyses, are systematically lower than those calculated from the XRD analyses (Table 2).

The CaO content is related to the carbonate minerals, mainly calcite (Fig. 5, Table 4). Based on the amount of calcite calculated from the bulk diffractograms, the corresponding amount

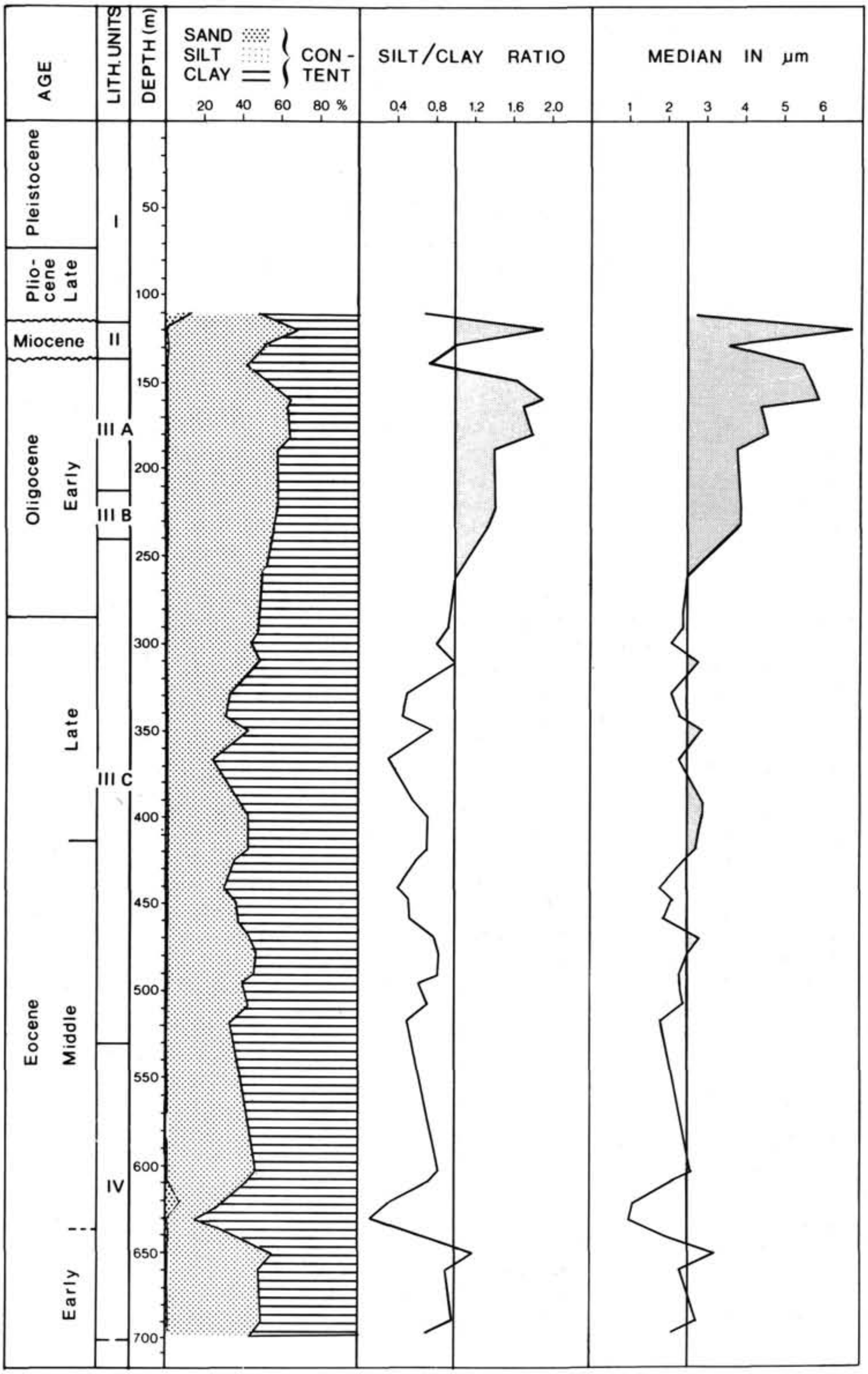

Figure 2. Grain-size distribution; percentages of sand, silt, clay, and the silt/clay ratio, as well as average grain size, and median.

of CaO is subtracted from the total CaO, and the remaining CaO is listed in Figure 5 and Table 5. We see that the content is very low and is probably related to clay minerals. The absolute values of noncarbonate-related CaO are not quite correct, as they were calculated from two different methods of quantification, not measured directly. The trends in the noncarbonate-related CaO variation are usually correct and generally show an upward-decreasing trend.

We believe that the MnO content (Fig. 5, Table 4) is incorporated in different types of mixed carbonates and also decreases upward (see Arthur et al., this volume). Certain horizons are distinctly MnO-enriched, especially in the lower part. The Na_2O

Table 1. Average parameters, age and lithologic units, and grain-size analyses of sediments at Site 647.

Depth (mbsf)	Number of samples	A/LU	Sand (wt%)	Silt (wt%)	Clay (wt%)	Silt/Clay ratio	Median (μm)
110	1	I	14.1	35.46	50.44	0.70	2.80
116–135.4	2	II	0.85	57.53	41.63	1.38	5.20
135.4–289	10	early Oligocene	0.27	56.93	42.77	1.33	4.26
135.4–212.3	6	IIIA	0.27	59.09	40.65	1.45	4.98
212.3–241.1	2	IIIB	0.42	57.88	41.70	1.39	3.90
289–415	9	late Eocene	0.26	39.26	60.47	0.65	2.52
415–640	16	middle Eocene	0.87	36.69	62.44	0.59	1.98
640–699	4	early Eocene	1.12	47.20	51.68	0.91	2.42

A/LU = age/lithologic unit.

content (Fig. 6, Tables 4 and 5) increases upward, probably from upward-decreasing compaction, which leads to an increasing amount of pore water. When dried for bulk analyses, halite precipitated on the sample and is responsible for the sodium content. The XRD bulk mineralogical analyses also showed higher contents of halite in the upper part of the horizon. Halite is not included in the quantitative distribution of the XRD bulk sediment minerals.

MgO content is fairly constant, between 2% and 3% (Fig. 6, Tables 4 and 5), except in the lowermost chlorite-containing sample, where the content is 6.2%. The nonchlorite related part of the MgO is probably present in smectites and mixed carbonates.

Al_2O_3 (Fig. 6, Tables 4 and 5) is relatively constant, between 10% and 15%, and originates mainly from the clay minerals and feldspars. Fe_2O_3 (Fig. 6, Tables 4 and 5) is relatively high, between 6% and 8%, and decreases slightly upcore. It is higher in the interval from 621 to 630 mbsf, where pyrite concretions are present. In this interval, the Fe_2O_3 content ranges up to 19%. We do not know whether the iron is present as divalent or trivalent ions, but the smectites of a dioctahedral type are probably the dominant source for the iron content, which infers a trivalent status. Iron oxides or oxyhydroxides are probably present, coating other mineral grains, although not in a well-crystallized phase, and are partly responsible for the sediment color. Minor amounts are present in the carbonates.

The K_2O content (Fig. 6, Tables 4 and 5) varies parallel to the illite content in the lower part of the sequence. It is also present in the feldspars.

DISCUSSION

Origin of Clay Minerals

The bulk geochemistry of the smectite-dominated clays, recalculated to a carbonate- and quartz-free basis, suggests a substitution of some aluminum with iron in the octahedral part of the crystal lattice (Table 6). The composition is similar to that of smectites from Paleocene/Eocene sedimentary clays derived from basaltic ash and smectites from *in-situ* transformations of volcanic ash layers, present in the North Sea Basin (Nielsen and Heilmann-Clausen, 1988). Yet, the North Sea smectites are somewhat more iron-rich and aluminum-poor than those from the Labrador Sea. Analyses from carbonate concretions in the lower part of this site (Bohrmann and Thiede, this volume) also indicate a nontronitic type of smectite minerals, which still is far from the pure nontronite end-member of the nontronite-beidellite series. Pure nontronites of hydrothermal origin are occasionally found in deep-sea sediments (Singer et al., 1984), with a significant amount of potassium in an interlayer position. The possible presence of potassium-smectites might explain the bad fit between potassium and illite, especially in the upper part of the hole. The slight upcore decrease in the iron contents, and particularly the manganese contents, the significant low Al_2O_3 content in the four lowermost, and particularly the two lowermost, samples, and the very small differences in geochemistry all suggest that only the few lowermost meters, from 699 to at least 696.7 mbsf, of sediment have been subjected to hydrothermal mineral transformations. From 689.9 mbsf to farther upcore, only thermal and almost isochemical transformations are present. No samples between 696.7 and 689.8 mbsf were analyzed. The smectite composition might be slightly less iron-rich upward, probably because the supply rate of iron and manganese decreased as the distance to the active rift increased through time.

We believe that kaolinite and illite originate mainly from continental areas supplied by suspensional transport. In analyses of the Labrador Shelf, Hiscott (1984) reported abundant kaolinite, illite, and chlorite, and less frequent smectites in Paleogene strata. In more distal locations, relative to the shoreline, the amount of detrital and coarser clay minerals, as for example kaolinite, illite, and probably chlorite, may be expected to diminish, with smectites expected to increase relatively. Results of analyses from this site agree fairly well with these expectations.

The cessation of seafloor spreading in the Labrador Sea in early Oligocene (Srivastava et al., 1981) is not marked by a distinct change in the clay composition at Site 647. Kaolinite and illite, however, increase slightly relative to smectites, and chlorite is present sporadically in the upper part of the early Oligocene. The change in clay mineralogy as a consequence of the end of spreading might have been more pronounced in younger Oligocene strata, which are absent in Site 647, probably because of erosion.

The increase in the quartz and feldspar contents in the upper part of the investigated sequence probably represents the initiation of a more immature and terrigeneous influenced sediment, delivered by melting icebergs. Textural, mineralogical, and chemical immature sediments, of the same age and transported by the same mechanism, are also reported by Hiscott et al., (this volume) in Baffin Bay. The presence of dropstones to a depth of 110 mbsf in this site is documented by Korstgard and Nielsen (this volume).

The Lowermost Sediment Record Above the Basalt

Quartz and calcite in veins and chlorite were reported in the transitional layer between the basalt and the sediment during shipboard description. The lowermost sample analyzed here contains abundant chlorite, and the iron (and particularly the magnesium) contents are accordingly higher than in the overlying sediments. Thus, we believe the chlorite was formed by a supply of magnesium- and iron-enriched, relatively hot water ascending from the basalt below through the newly formed sediment. The water and its dissolved components reacted with the original smectitic components, which led to *in-situ* formation of chlorite.

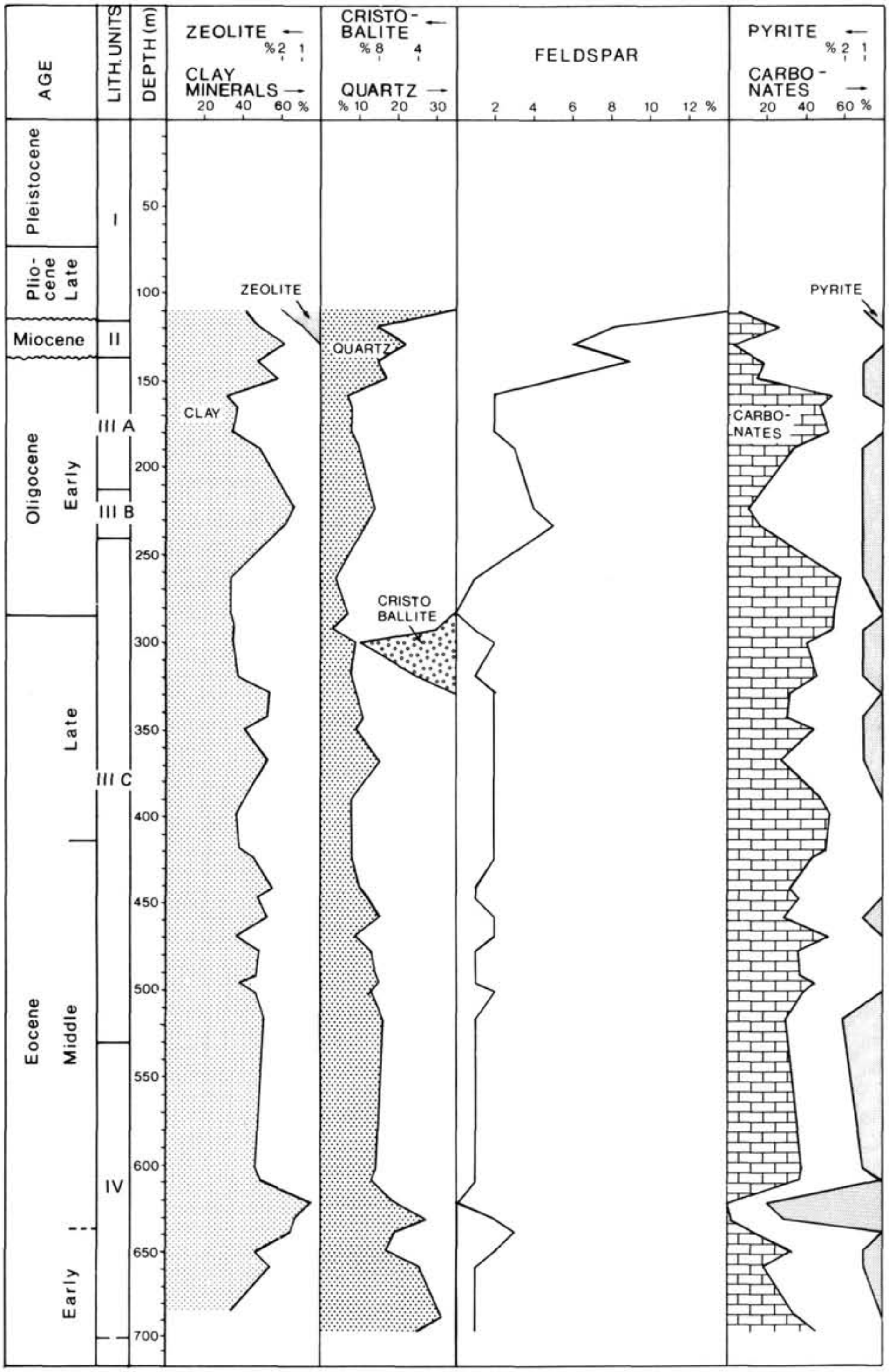

Figure 3. Bulk mineralogical composition, indicating carbonates, clay minerals, quartz, feldspars, cristobalite, zeolite, and pyrite.

The calculated illite content is also higher in the two lowermost samples than was observed higher in the section. This interpretation may be partially incorrect, but is a consequence of the identification criteria, which do not allow an accurate distinction between different mineral phases with crystal-lattice dimensions of 10 Å. The calculated illite-content may include original smectites, which have irreversibly lost interlayer water and, consequently, swelling capacity as a result of the abnormally high temperatures penetrating upward from the underlying basalt. The higher illite percentages in the lowermost two samples are not accompanied by higher potassium contents, in contrast to, for example, the interval from 620–640 mbsf, where both the illite and potassium contents are correspondingly higher.

The irreversible thermal destruction of the swelling ability of smectites normally takes place at temperatures in the magnitude of 500°–800°C (Grim, 1968). For pure nontronites, the process

Table 2. Average parameters, age and lithologic units, and mineralogy of bulk sediments, determined by X-ray diffraction.

Depth (mbsf)	Number of samples	A/LU	Clay (%)	QUA (%)	FSP (%)	CAR (%)	LCAR (%)
110	1	I	42	34	14	6	2
116–135.4	2	II	55	19	7	15	8
135.4–289	10	early Oligocene	46	10	3	36	27
135.4–212.3	6	IIIA	43	11	4	37	26
212.3–241.1	2	IIIB	64	13	5	14	10
289–415	9	late Eocene	43	9	2	42	37
415–640	16	middle Eocene	50	14	1	34	28
640–699	4	early Eocene	45	24	2	26	21

A/LU = age and lithologic units; QUA = quartz; FSP = feldspar; CAR = total amount of carbonate minerals; and LCAR = CO_2 detected in LECO induction-furnance, recalculated to $CaCO_2$.

starts at about 400°C. Three samples from the Eocene section of this site were heated to progressively elevated temperatures in steps of 25°C and in periods varying from 2 hr to 7 weeks, with intervening glycollation and diffraction analyses to trace the temperature needed for destroying swelling ability. We found this temperature to be 550°C, which we believe is much higher than the maximum temperature these sediments have ever been subjected to, even for the two lowermost samples, about 2 and 10 m above the surface of the basalt, respectively. The extremely longer period during which the sediments have been exposed to higher temperatures compared to laboratory tests might be the most reasonable explanation. Yet, note that elevated temperatures might have destroyed the swelling ability in smectites 2 m above the basalt, equivalent to 80,000 yr after basalt formation, and partly destroyed it 10 m above, equivalent to 400,000 yr after basalt formation. The lowermost unaffected sample is situated about 30 m above the basalt, equivalent to 1.2 m.y.

In the normal diagenetic evolution of clay-rich sediments, the smectite transformation to illite, if there is enough potassium, or to chlorite if there is enough magnesium or it is supplied from beneath, takes place in temperatures ranging from 100° to 200°C (Segonzac, 1970), normally through mixed-layer mineral phases. Temperatures of this magnitude probably were reached soon after basalt formation at this site.

Besides these hydrothermal chlorites and thermal illites, no indication of distinct diagenetic mineral changes exists in the clay minerals. The composition changes very little throughout the Paleogene sequence. This also seems to be the case in the carbonate concretions, which are probably a relatively early diagenetic phenomenon (Arthur et al., this volume; Bohrmann and Thiede, this volume).

CONCLUSIONS

This investigation has shown the following conclusions:

1. The composition of the Paleogene sediments, from 135.4 to 699 mbsf, varies only a little throughout the sequence, except for the lower 30 m.
2. The compositional variations mostly result from variations in the composition and amount of biogenic components.
3. Diagenetic mineral transformations seem mainly to influence the amount and composition of the carbonates and the amount of pyrite.
4. Detrital minerals, such as quartz, feldspars, kaolinite, and illite, are present only in small amounts.
5. In the lowermost 30 m, hydrothermal activity is responsible for chlorite formation in the transitional layer between the basalt and the sediment. Above this relatively thin zone, thermal diagenesis is responsible for a reduction in the swelling ability of the authigenic nontronitic smectites, which are the dominant mineral in the Paleogene.

ACKNOWLEDGMENT

Financial support was provided by the Danish Natural Science Research Council, Grant No. J 81-5289.

REFERENCES

Biscaye, P. E., 1965. Mineralogy and sedimentation of Recent deep-sea clays in the Atlantic Ocean and adjacent seas and oceans. *Geol. Soc. Am. Bull.*, 76:803–832.

Brindley, G. W., and Brown, G., 1980. Crystal structures of clay minerals and their X-ray identification. *Mineral. Soc. Mono.*, 5:1–495.

Gibbs, R. W., 1971. X-ray diffraction mounts. *In* Carver, R. (Ed.), *Procedures in Sedimentary Petrology*: New York (Wiley-Interscience), 531–539.

Grim, R. E., 1968. *Clay Mineralogy*: New York (McGraw-Hill), 2nd Edit, 1–596. Hiscott, R. N., 1984. Clay mineralogy and clay-mineral provenance of Cretaceous and Paleogene strata, Labrador and Baffin shelves. *Bull. Can. Pet. Geol.*, 32(3):272-280.

Johns, W. D., Grim, R. E., and Bradley, W. F., 1954. Quantitative estimation of clay minerals by diffraction methods. *J. Sediment. Petrol.*, 24:242–251.

Nielsen, O. B., and Heilmann-Clausen, C., 1988. Palaeogene volcanism: the sedimentary record in Denmark. *In* Morton, A. C., and Lindsay, L. M. (Eds.), *Early Tertiary Volcanism and the Opening of the NE Atlantic.* Geol. Soc. London Spec. Publ. 39:395–405.

Schultz, L. G., 1964. Quantitative interpretation of mineralogical composition from X-ray and chemical data for the Pierre Shale. *U.S. Geol. Survey Prof. Pap.*, 391-C:1–31.

de Segonzac, G. D., 1970. The transformation of clay minerals during diagenesis and low-grade metamorphism: a review. *Sedimentology*, 15:281–346.

Singer, A., Stoffers, P., Heller-Kallai, L., and Szafranek, D., 1984. Nontronite in a deep-sea core from the South Pacific. *Clays and Clay Minerals*, 32:375–383.

Srivastava, S. P., Arthur, M., et al., 1987. *Proc. ODP, Init. Repts.*, 105: College Station, TX (Ocean Drilling Program), 917.

Srivastava, S. P., Falconer, R.K.H., and MacLean, B., 1981. Labrador Sea, Davis Strait, Baffin Bay: geology and geophysics—a review. *In* Kerr, J. W., and Fergusson, A. J. (Eds.), *Geology of the North Atlantic Borderlands.* Can. Soc. Pet. Geol. Mem., 7:333–398.

Date of initial receipt: 7 January 1987
Date of acceptance: 22 June 1988
Ms B105-116

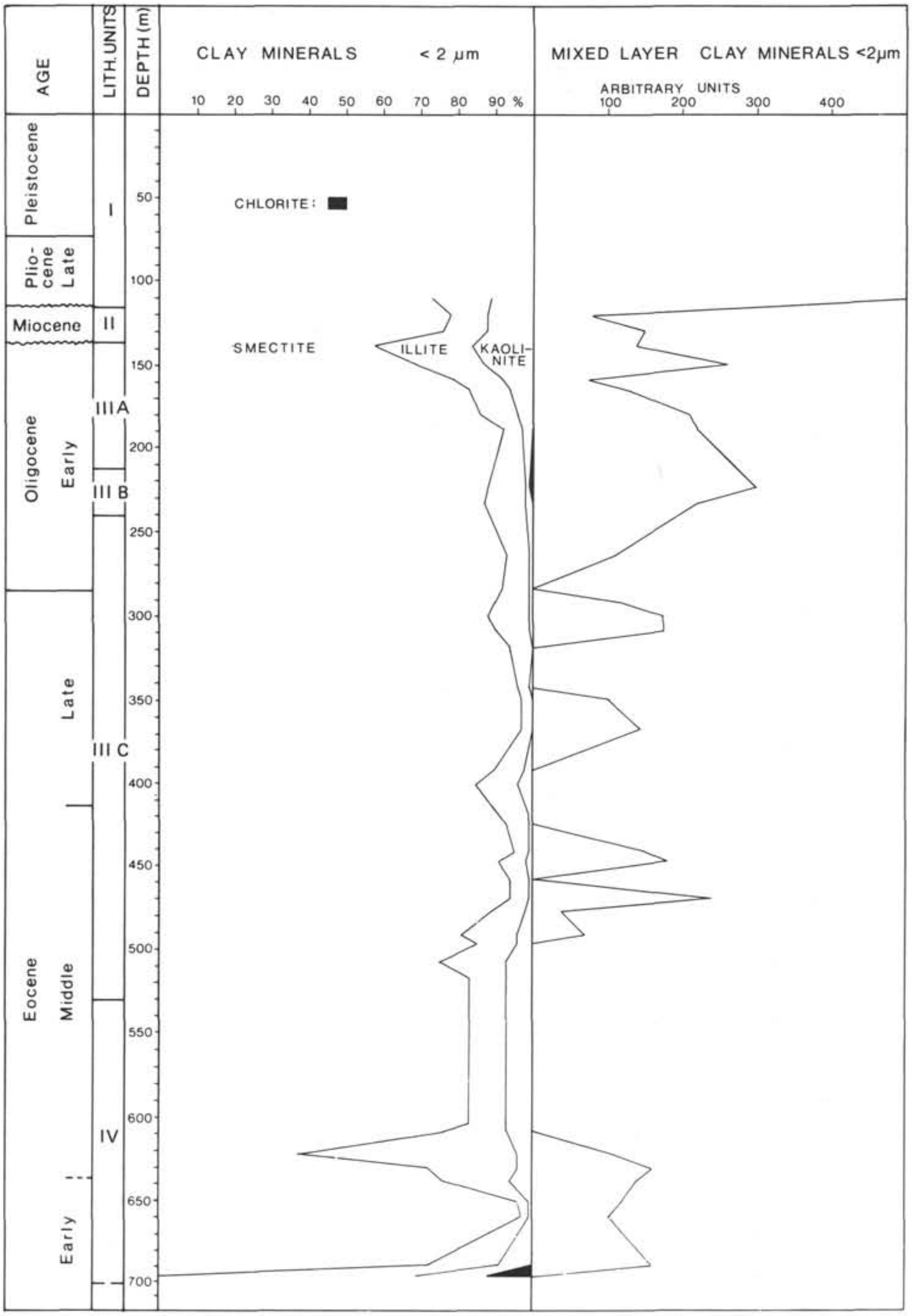

Figure 4. Clay mineralogy; quantitative distribution of clay minerals in the clay fraction (<2 µm).

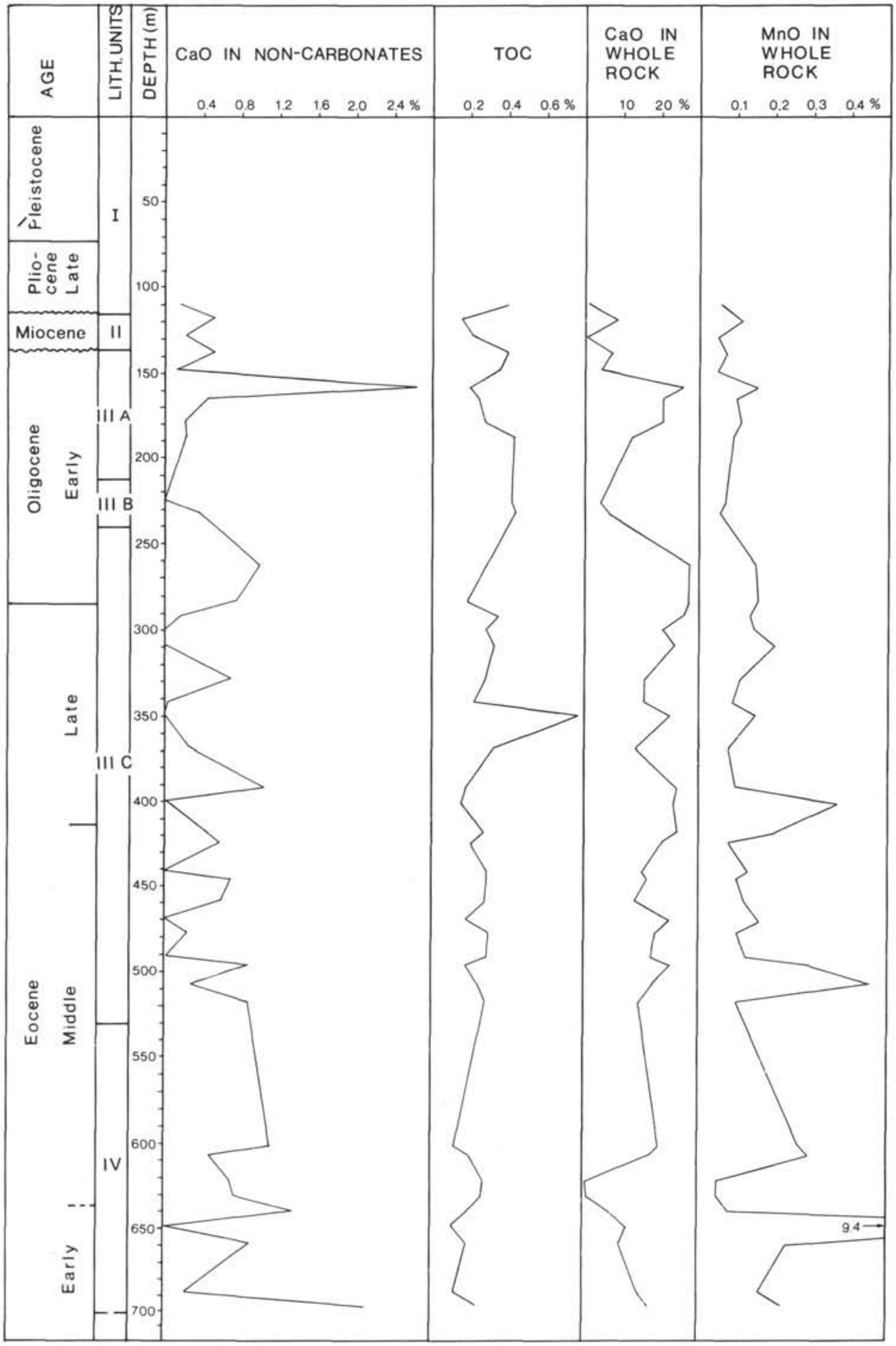

Figure 5. Geochemistry showing TOC, total CaO, total MnO, and CaO in noncarbonates.

Table 3. Average parameters, age and lithologic units, and mineralogy of the clay fraction.

Depth (mbsf)	Number of samples	A/LU	SME (%)	ILL (%)	KAO (%)	CHL (%)	MIX
110	1	I	73	16	11	0	500
116–135.4	2	II	77	12	12	0	115
135.4–289	10	early Oligocene	83	12	6	0	167
135.4–212.3	6	IIIA	78	14	8	0	173
212.3–241.1	2	IIIB	87	10	2	1	260
289–415	9	late Eocene	92	7	1	0	80
415–640	16	middle Eocene	82	14	4	0	63
640–699	4	early Eocene	68	22	7	2	104

A/LU = age/lithologic unit; SME = smectite; ILL = illite; KAO = kaolinite; CHL = chlorite; MIX = area in arbitrary units of the basal reflection from mixed-layer clay minerals.

Table 4. Average parameters, age and lithologic units, and chemical composition of bulk sediments.

Depth (mbsf)	Number of samples	A/LU	CaO (%)	MnO (%)	MgO (%)	K_2O (%)	Fe_2O_3 (%)	Na_2O (%)	Al_2O_3 (%)	TOC (%)
110	1	I	1.44	0.061	2.26	2.70	5.76	2.50	14.74	0.40
116–135.4	2	II	4.95	0.081	2.73	2.36	6.91	2.95	13.82	0.18
135.4–289	10	early Oligocene	15.79	0.103	2.02	1.55	5.26	2.68	10.15	0.33
135.4–212.3	6	IIIA	15.30	0.098	2.12	1.59	5.21	2.97	10.12	0.32
212.3–241.1	2	IIIB	5.29	0.065	2.36	1.77	6.34	3.09	12.23	0.43
289–415	9	late Eocene	20.59	0.156	1.47	1.46	4.68	1.36	9.64	0.32
415–640	16	middle Eocene	16.13	0.171	1.74	1.86	6.92	1.14	10.18	0.24
640–699	4	early Eocene	11.25	2.02	2.66	1.97	5.27	0.90	8.54	0.16

A/LU = age/lithologic unit; TOC = total organic carbon.

Table 5. Average parameters, age and lithologic units, and chemical composition recalculated to percentage of the noncarbonate mineral content.

Depth (mbsf)	Number of samples	A/LU	CaO (%)	MgO (%)	K_2O (%)	Fe_2O_3 (%)	Na_2O (%)	Al_2O_3 (%)
110	1	I	0.18	2.31	2.76	5.90	2.56	15.08
116–135.4	2	II	0.35	2.95	2.59	7.59	3.16	15.14
135.4–289	10	early Oligocene	0.56	2.77	2.13	7.31	3.65	14.03
135.4–212.3	6	IIIA	0.70	2.86	2.13	7.06	4.05	13.65
212.3–241.1	2	IIIB	0	2.61	1.96	7.03	3.42	13.55
289–415	9	late Eocene	0	2.34	2.32	7.46	2.17	15.30
415–640	16	middle Eocene	0.48	2.38	2.51	9.02	1.62	14.22
640–699	4	early Eocene	0	3.38	2.46	6.61	1.13	10.63

A/LU = age/lithologic unit.

Table 6. Average parameters, age and lithologic units, and chemical composition recalculated to carbonate- and quartz-free basis.

Depth (mbsf)	Number of samples	A/LU	Al_2O_3 (%)	Fe_2O_3 (%)	K_2O (%)	MgO (%)
110	1	I	24.57	9.60	4.50	3.76
116–135.4	2	II	20.94	10.47	3.58	4.14
135.4–289	10	early Oligocene	18.80	9.74	2.87	3.74
135.4–212.3	6	IIIA	19.46	10.02	3.06	4.08
212.3–241.4	2	IIIB	16.75	8.68	2.42	3.23
289–415	9	late Eocene	19.67	9.55	2.98	3.00
415–640	16	middle Eocene	19.58	13.31	3.58	3.35
640–699	4	early Eocene	17.08	10.58	3.94	5.32

A/LU = age/lithologic unit.

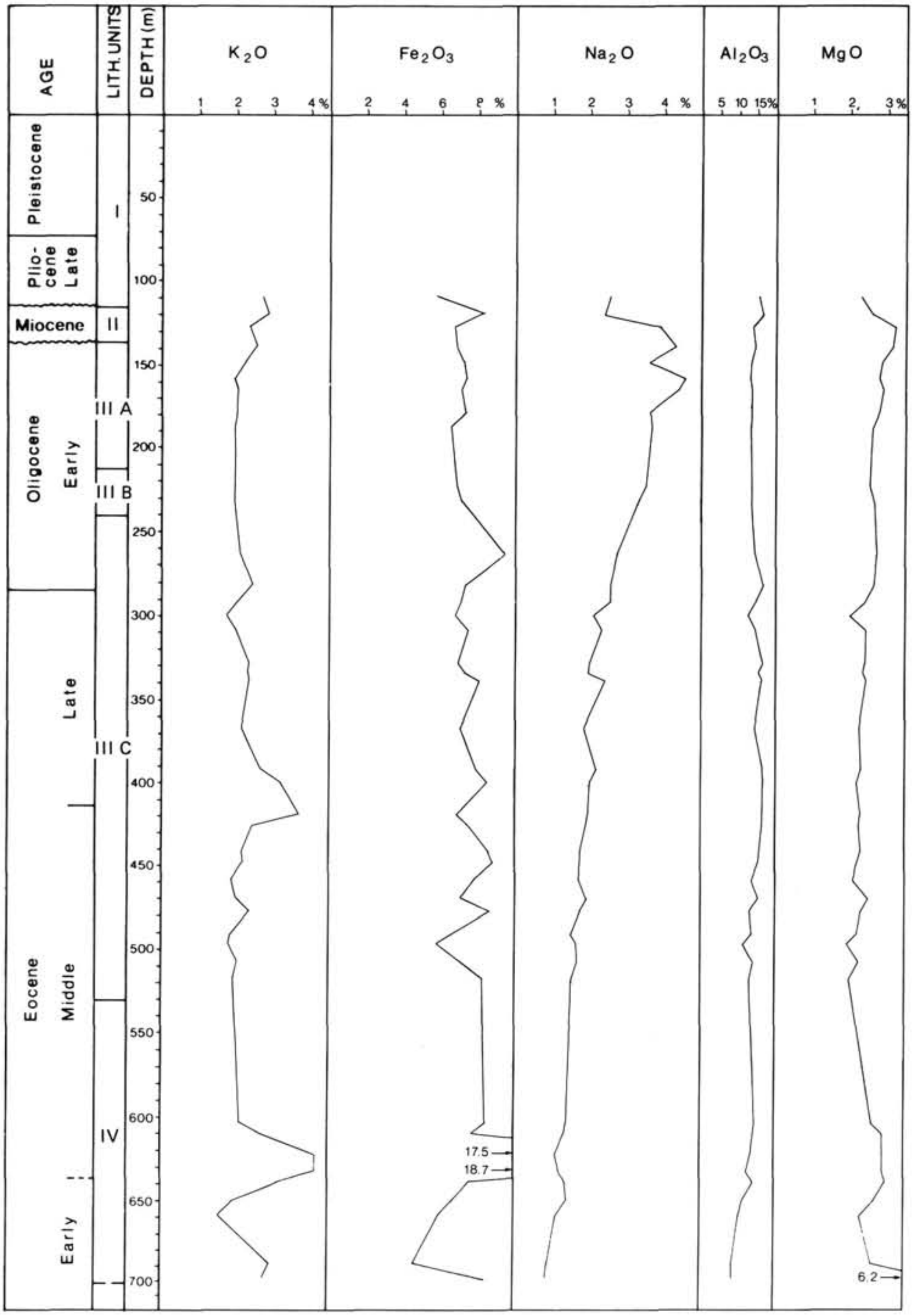

Figure 6. Geochemistry showing contents of AL_2O_3, Fe_2O_3, Na_2O, K_2O, and MgO; recalculated to carbonate-free basis.